J. Membrane Biol. 146, 327–341 (1995)

The Journal of
Membrane
Biology

Two Types of A-Channels in Lymnaea Neurons

S.I. Alekseev,[1] M.C. Ziskin[2]

[1]Institute of Cell Biophysics, Russian Academy of Sciences, Puschino, Moscow Region, Russia
[2]Center for Biomedical Physics, Temple University Medical School, Philadelphia, PA 19140

Received: 31 October 1994/Revised: 4 April 1995

Abstract. The gating mechanism of A-channels of *Lymnaea* neurons and the effect of tetraethylammonium (TEA) on these channels were studied using macroscopic recording techniques. Along with the fast-inactivating A-current (I_{af}) described earlier we found a slow-inactivating A-current (I_{as}) in some neurons of the visceral ganglion. Both currents have revealed similar activation kinetics, but differ in the inactivation kinetics and mechanisms. The inactivation kinetics of I_{as} were satisfactorily described by a sum of two exponentials with rate constants (τ^{-1}) of 28 s^{-1} and 4.5 s^{-1} at V = −20 mV. Intracellular TEA reduced the peak amplitudes of I_{af} and I_{as} and slowed the rate of the fast phase of inactivation of I_{af}. This resulted in a crossover of the current traces in the presence and absence of TEA, as though it competes with the binding of the inactivating particle. The mechanism of the fast phase of inactivation of I_{af} is similar to that of fast inactivation of the *Shaker* K^+ channels which appears to be due to a ball-and-chain mechanism. The slow phases of inactivation of I_{af} and I_{as} reveal properties characteristic of C-type inactivation shown in *Shaker* K^+ channels. A partially coupled model including three pathways for transition of a channel from the closed to open states accurately reproduces all of the experimental data. It has voltage-independent transitions to the inactivation states indicating that inactivation of A-current is not associated with charge movement through the membrane. The results suggest that *Lymnaea* A-channels seem to be heteromultimeric.

Key words: *Lymnaea* neurons — A-currents — Tetraethylammonium blockade — Kinetic model

Correspondence to: M.C. Ziskin

Introduction

The fast-inactivating A-current (I_{af}) in *Lymnaea* neurons has been described earlier in great detail (Alekseev & Zaykin, 1993). This current decays with multiple exponential components suggesting multiple inactivation processes. At a potential range from −90 to −60 mV, I_{af} can undergo slow inactivation from the closed states of the channel. The fast phase of inactivation shows a complex voltage dependence which can not be described by the known kinetic schemes developed for modeling of inactivation of the fast potassium channels (Solc & Aldrich, 1990; Zagotta & Aldrich, 1990; Hoshi, Zagotta, & Aldrich, 1991). In many other instances I_{af} reveals properties similar to those of the *Shaker* potassium currents (Hoshi et al., 1991).

Using site-directed mutagenesis, Hoshi, Zagotta, & Aldrich (1990), Zagotta, Hoshi, & Aldrich (1990), and Hoshi et al. (1991) have shown that the fast (N-type) and slow (C-type) components of inactivation of the *Shaker* K^+ channels are caused by two distinct molecular mechanisms. N-type inactivation involves the amino terminus of the channel protein in a "ball-and-chain" type of arrangement initially proposed by Armstrong and Bezanilla (Armstrong & Bezanilla, 1977; Bezanilla & Armstrong, 1977); and later this mechanism was directly confirmed in the experiments with *Shaker* K^+ channels (Hoshi et al., 1990; Zagotta et al., 1990). C-type inactivation occurs in channels that have N-type inactivation disrupted, and does not use a ball-and-chain mechanism (Hoshi et al., 1991). Tetraethylammonium (TEA), a well-known blocker of potassium channels (Armstrong & Binstock, 1965; Armstrong & Hille, 1972), interacts in a specific way with the inactivation gates. It produces a substantial slowing of the fast inactivation due to competition with the inactivation particle ("ball") for binding to the same site at the inner mouth of the channel (Choi, Aldrich, & Yellen, 1991). Lately TEA has been

widely used for identifying amino acids which make up the inner wall of the pore (Yellen et al., 1991; Choi et al., 1993).

The main aim of this study was to develop a quantitative model of *Lymnaea* A-channels describing complex inactivation kinetics of the macroscopic currents. As the potential dependence of inactivation in *Shaker* K^+ channels results from that of activation (Zagotta & Aldrich, 1990) we first investigated the activation kinetics and the effects of Ca^{2+} and H^+ on these kinetics. The model was then tested to see if the changes in only the activation parameters could reproduce the effects of Ca^{2+} and H^+ on the inactivation kinetics. To identify the inactivation mechanisms similar to N-type inactivation, we used TEA specifically interacting with the fast inactivation gate. Along with the fast-inactivating current, I_{af}, described earlier (Alekseev & Zaykin, 1993), we have also found a slow-inactivating current, I_{as}, in the giant neurons of the visceral ganglion. A comparative analysis of the activation parameters of the fast- and slow-inactivating currents shows that both types of currents are activated in a similar way. The results of experiments with TEA are consistent with the suggestion of different mechanisms underlying inactivation of A-currents. A model was derived for activation and inactivation gating based on the studies of macroscopic kinetics. It includes three opening pathways for a channel. The voltage-dependent transitions between these pathways determine the complex voltage dependence of the fast phase of inactivation.

Materials and Methods

Pronase and tris(hydroxymethyl)aminomethane (TRIS) were obtained from Sigma Chemical (St. Louis, MO), and tetraethylammonium chloride was obtained from Aldrich Chemical (Milwaukee, WI).

The experiments were performed on internally perfused neurons from the right and left parietal and visceral ganglia of *Lymnaea stagnalis* maintained at 20–22°C. The methods employed for isolation of neurons, for intracellular perfusion, current identification, and curve fitting followed those described in detail elsewhere (Alekseev, 1992).

Macroscopic currents were recorded using a whole-cell voltage-clamp technique (Alekseev, 1992). A polythene pipette with a pore of 40–50 μm in diameter served as a suction electrode. Series resistance, R_s, formed mainly by the ohmic resistance of the pore was 100–120 kΩ. It was partially compensated electronically. For the current amplitudes in these experiments, voltage errors due to R_s did not exceed a few millivolts. A new level of the membrane potential could be achieved in 100–150 μsec (estimated from the potential settling time).

To isolate A-currents from Na^+-current, NaCl was omitted from the external solutions. Twenty mM TEA was added to depress both the delayed rectified and Ca^{2+}-activated K^+ currents. Separation of A-currents from the remaining currents, including capacitive transient currents and leakage currents, was done by subtracting traces recorded without prepulses of −150 mV (Alekseev, 1992). The inactivation kinetics at subthreshold potentials (from −100 to −60 mV) were obtained by using a double-pulse method, i.e., the decay of the peak current was measured following a test pulse as a function of the preceding conditioning pulse duration.

Table 1. Composition of the external solutions (mM)

Solution	KCl	$CaCl_2$	$MgCl_2$	TEA	TRIS	pH
N1	1.6	2	4	0	76	7.5
N2	1.6	2	4	20	56	7.5
N3	1.6	2	16	20	32	7.5
N4	1.6	16	2	20	32	7.5
N5	1.6	2	4	20	66	7.5

In most of the experiments, the internal standard solution contained 80 mM KCl and 10 mM TRIS-HCl (pH 7.3). In experiments with TEA, the internal control solution with 80 mM KCl and 20 mM TRIS-HCl (pH 7.3) was replaced with a solution containing 20 mM TEA, 80 mM KCl and 2 mM TRIS-HCl (pH 7.3). The compositions of the external solutions are given in Table 1. In a study of the calcium and magnesium effects, the sum of the concentrations of these ions in the external solution was kept constant (solutions N3 and N4). TEA was added to all the solutions to decrease the possible contamination of A-currents with the delayed potassium current.

Results

Two Types of A-Currents

The fast-inactivating A-current in *Lymnaea* neurons has already been described in literature (Alekseev, 1992; Alekseev & Zaykin, 1993). The inactivation kinetics of this current were described by a sum of three exponentials with rate constants (τ^{-1}) of $\gamma_f = 80\ s^{-1}$, $\gamma_2 = 30\ s^{-1}$, $\gamma_3 = 5\ s^{-1}$ at $V = 0$ mV. Figure 1*A* shows the records of the current at different potentials. Similar A-currents are usually recorded in most neurons of the right and left parietal ganglia.

The slow-inactivating A-current occurred in several giant neurons of the visceral ganglion but never in the right and left parietal ganglia. It was found to have a much smaller amplitude than that of the fast-inactivating current for any given voltage (Fig. 1*B*). The inactivation kinetics of I_{as} can be adequately described as the sum of two exponentials. Figure 2 shows the rate constants over a wide range of voltage (from −90 to +40 mV). From −40 to +40 mV, inactivation rate of I_{as} has little dependence on voltage. The steady-state inactivation ($V_o = -98 \pm 5$ mV, $d = 6.2 \pm 0.2$ mV) and time course of removal from inactivation ($\gamma_f = 15\ s^{-1}$ at $V = -120$ mV) of I_{as} closely resemble those of I_{af}.

It is suspected that the different phases of inactivation of I_{af} may be resulting from individual inactivation of two completely different channels. To check this, we carried out the following experiment. First, a test pulse of 0 mV was applied to the membrane for 100 msec to complete fast inactivation. At the end of the pulse we observed only a slow-inactivating current of small amplitude. Then the membrane potential was changed to

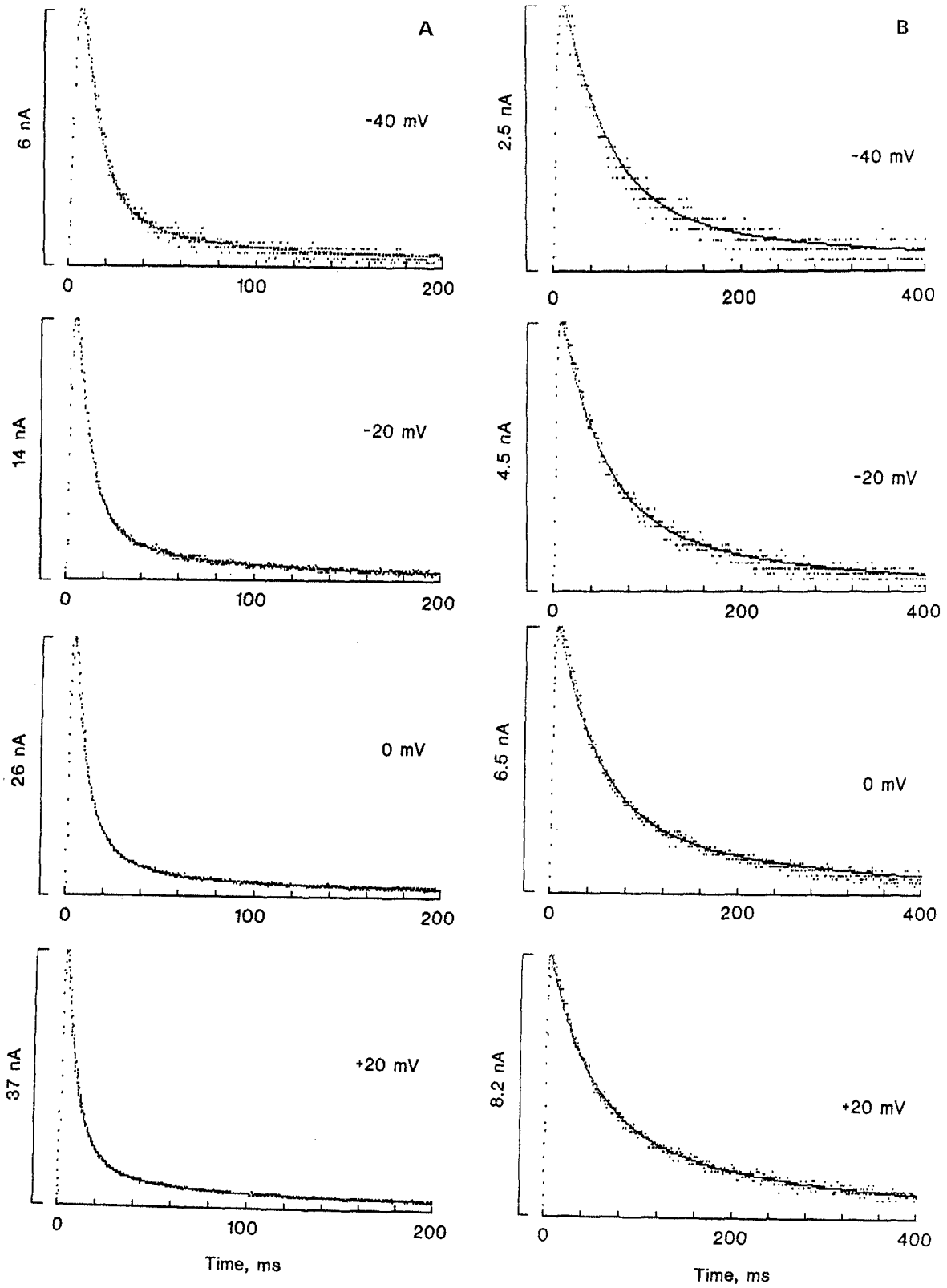

Fig. 1. Fast-inactivating (*A*) and slow-inactivating (*B*) A-currents in response to step depolarizations indicated with preceding hyperpolarizing pulses of 200 msec duration to −150 mV. Superimposed traces show the computer-drawn currents generated from the kinetic scheme 6 (*A* traces) and scheme 7 (*B* traces). I_{af} and I_{as} records were obtained in external solution N2.

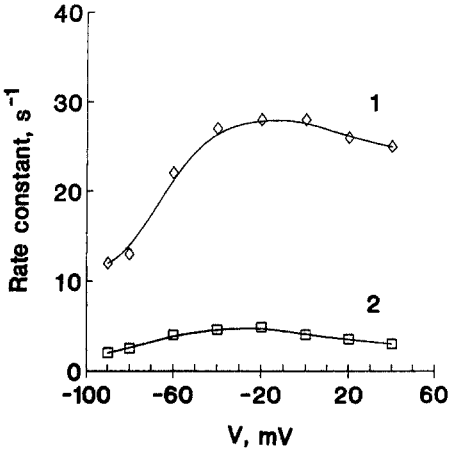

Fig. 2. Rate constants (τ^{-1}) of slow-inactivating A-current as a function of voltage. Rate constants, 1 and 2, were calculated using a two-exponential fit to the inactivation kinetics. I_{as} records were made in external solution N2.

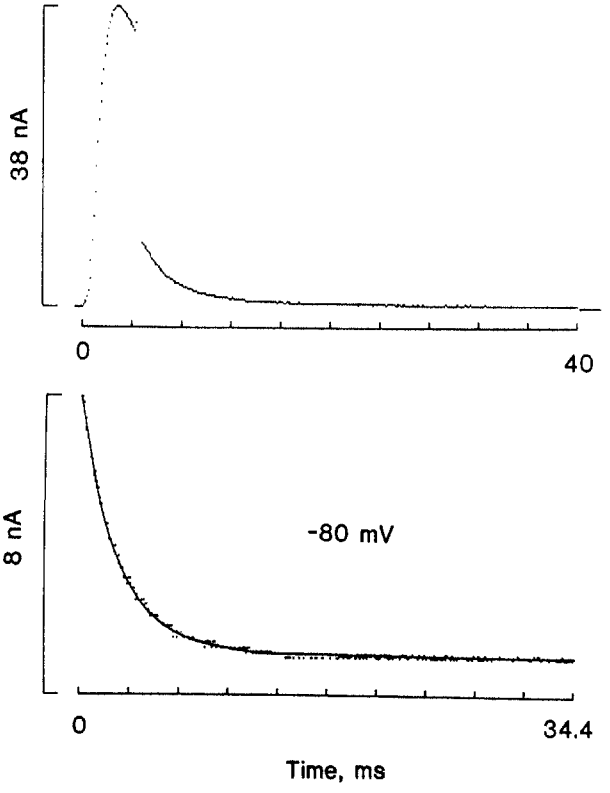

Fig. 3. Tail current kinetics of the fast-inactivating current. Upper trace shows an example of a recording of tail current. Depolarizing pulses (4 msec) to +20 mV with preceding hyperpolarizing pulses of 200 msec duration to −150 mV were given to activate the channels, followed by repolarization to different potentials. The bottom trace shows tail kinetic in external solution N3 at −80 mV. The smooth line represents the computer-estimated values from scheme 1.

−75 mV for 40 msec and brought back to 0 mV. In this case, we again observed a current with the same amplitude as before but containing the fast and slow phases of inactivation. In a preliminary experiment, no removal from inactivation of I_{af} was found for 40 msec at −75 mV. This means that the channels remaining in the open state after fast inactivation demonstrate the same ability for inactivation as those already inactivated. Hence, in the studied neurons mainly one type of channel displays both phases of inactivation of I_{af}.

Activation Kinetics

The great difference between the rates of activation and inactivation allows one to calculate accurately the parameters of inactivation kinetics $h(t)$. Earlier the activation kinetics of a sodium channel were derived by dividing the measured current values by the inactivation variable: $I(t)/h(t)$ (Keynes & Rojas, 1976; Oxford, 1981). Though this method assumes that activation and inactivation are independent, their kinetics were better described using a coupled model (Armstrong & Bezanilla, 1977; Bezanilla & Armstrong, 1977). Moreover, the activation kinetics obtained by the same method with inactivation intact were compared with those obtained after removal of inactivation with pronase (Oxford, 1981). Results with and without pronase were similar, and therefore provide a rationale for the calculation of the A-current activation kinetics obtained by dividing the current by $h(t)$.

The activation kinetics in the potential range of −30 to +10 mV were satisfactorily approximated by the Hodgkin-Huxley (HH) expression for a potassium current as n^4 (Hodgkin & Huxley, 1952). But in a wider potential range the quality of approximation became progressively worse. To solve this problem, we have described the rising phase of the activation kinetics by an exponential function of the type:

$$I = I_o(1 - \exp(-t/\tau_a)), \quad (1)$$

where I_o is the maximum current, and τ_a is the activation time constant. In this case, the quality of approximation was good over a wide potential range.

Following a depolarizing prepulse that activated most of the channels, a step repolarization to a more negative potential caused a current decay which is referred to as a tail current or a deactivation (Fig. 3). In order to reduce the influence of inactivation on the accuracy of determination of the deactivation time constant, τ_d, we used the current tails obtained in the potential range from −70 to −100 mV. The deactivation kinetics in this potential range have been approximated with single-exponential expression.

Values of τ_a and τ_d determined as described above are shown as a function of potential in Fig. 4. As can be seen, there is a good agreement between values of τ_a and

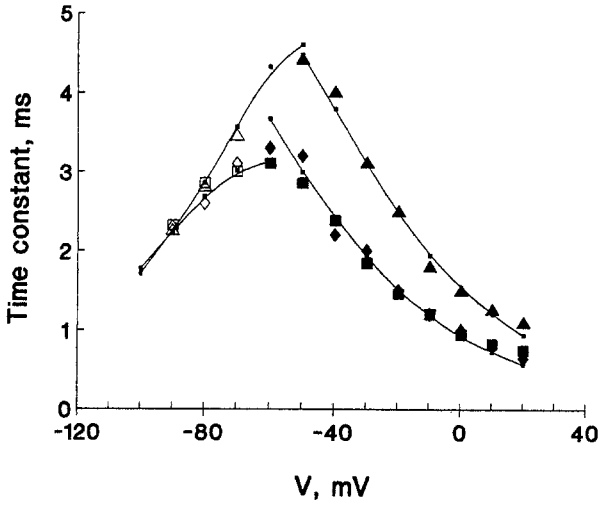

Fig. 4. Time constants of activation (filled symbols) and deactivation (open symbols) of A-currents as a function of voltage. The data were computed using a one-exponential fit to the rising phase of the activation kinetics, $I(t)/h(t)$, and tail current kinetics. Squares and triangles correspond to measurements of the fast-inactivating current kinetics in the external solution N3 and N4, respectively. Diamonds are measurements of the slow-inactivating current kinetics in the external solution N3. Dots are calculated values using scheme 1 for each membrane potential. The curves are drawn through the dots by hand. The experimental data shown are close to the mean magnitudes of τ_a and τ_d. Standard deviations did not exceed ±15%.

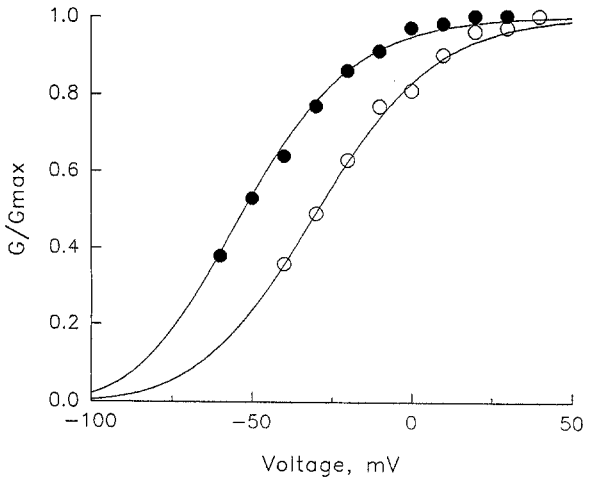

Fig. 5. Effect of divalent cations on the steady-state conductance curve of I_{af}. Filled and open circles are normalized conductances in the external solutions N3 and N4, respectively. The steady-state probabilities of the channel being open were computed using Eq. 5 (continuous lines). Increase in the calcium concentration from 2 to 16 mM causes a positive shift of the normalized conductance curve by 21 mV.

τ_d of the fast- and slow-inactivating currents. The temperature coefficient Q_{10} for τ_a and τ_d was found to be 3.0 ± 0.1 (four experiments).

The dependence of the channel conductance of both the fast- and slow-inactivating currents on potential are equally well described by a Boltzmann distribution:

$$G/G_{\max} = (1 + \exp[(V_o - V)/d])^{-1} \quad (2)$$

where G is the conductance in response to some depolarizing potential V and equal to $I_a/(V - E_r)$, $G_{\max}$ is the maximum conductance, V_o is the value of the potential when $G/G_{\max} = 0.5$, d is the slope factor describing the steepness of the activation curve, E_r is the reversal potential of the A-channels. The value of E_r for both types of current estimated from the instantaneous V-I relation was −100 mV. For the eight studied cells, $V_o = -48 \pm 8$ mV, $d = 17 \pm 2$ mV. Plots of $G(V)/G_{\max}$ are shown in Fig. 5.

Effect of Divalent Ions

An equimolar substitution of 2 mM Ca^{2+} and 16 mM Mg^{2+} (solution N3) for 16 mM Ca^{2+} and 2 mM Mg^{2+} (solution N4), resulted in an appreciable decrease in the amplitude and the activation rate of the fast-inactivating current (Fig. 6). The magnitudes of these changes depended on the potential and were manifested primarily in the parallel positive shifts of curves $\tau_a(V)$ (Fig. 4) and $G(V)/G_{\max}$ (Fig. 5) by 22 ± 2 mV and by 21 ± 2 mV, respectively. At the same time, deactivation kinetics were insensitive to this replacement (Fig. 4). The effect of the replacement of divalent ions on fast inactivation was more complex (Alekseev & Zaykin, 1993). A part of the $\gamma_f(V)$ curve on the left of the plateau and the steady-state inactivation curve were shifted by 23 ± 4 and 21 ± 3 mV, respectively, in the depolarizing direction. As can be seen, the shifts of $\tau_a(V)$ and $G(V)/G_{\max}$ curves are within the range of shifts of $\gamma_f(V)$ and steady-state inactivation curves.

TEA Blockade

Figure 7 shows the changes in the fast-inactivating current affected by 20 mM external TEA. The external TEA resulted in a decrease of the current amplitude by approximately 25% and a parallel shift of the steady-state activation and inactivation curves by 10 ± 2 mV in the depolarizing direction. The voltage dependencies of the rate constants of activation and inactivation show a similar shift. These changes, except for the shifts of the voltage-dependent parameters of current, are similar to those described earlier for the effect of external TEA on the potassium channels (Choi et al., 1991).

During perfusion of a neuron with internal solution containing 20 mM TEA, the amplitude of I_{af} at the membrane potential of −20 mV decreased by half of its initial value within approximately 40 min. At the same time the inactivation rate decreased noticeably causing

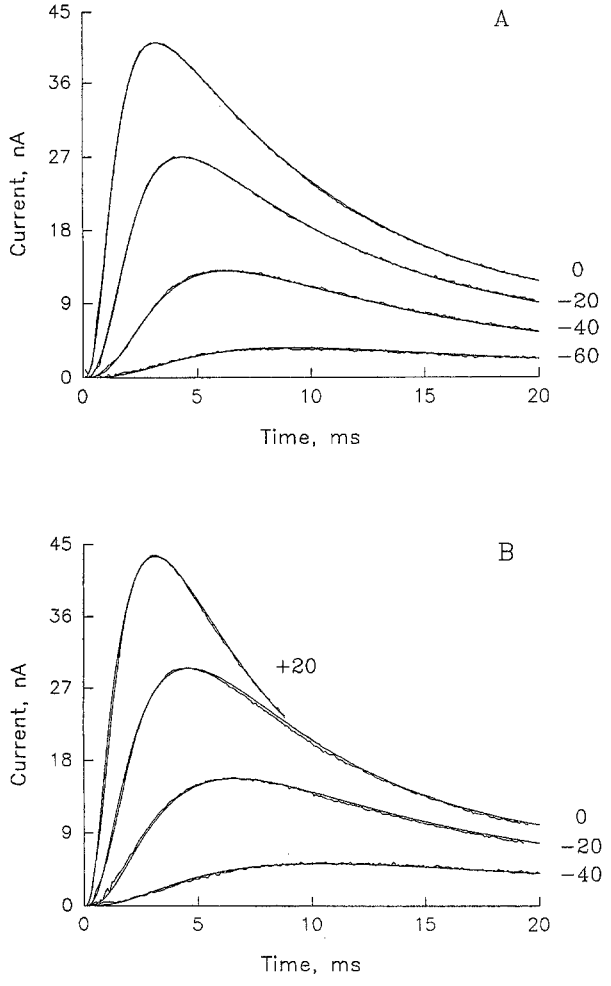

Fig. 6. Effect of divalent ions on I_{af}. The currents were recorded in solution N3 containing 2 mM Ca^{2+} and 16 mM mg^{2+} (*A*) and in the solution N4 containing 16 mM Ca^{2+} and 2 mM Mg^{2+} (*B*). The test potential (in millivolts) is given on the right side of each trace. Superimposed on the data are the fits of scheme 6 to the kinetics.

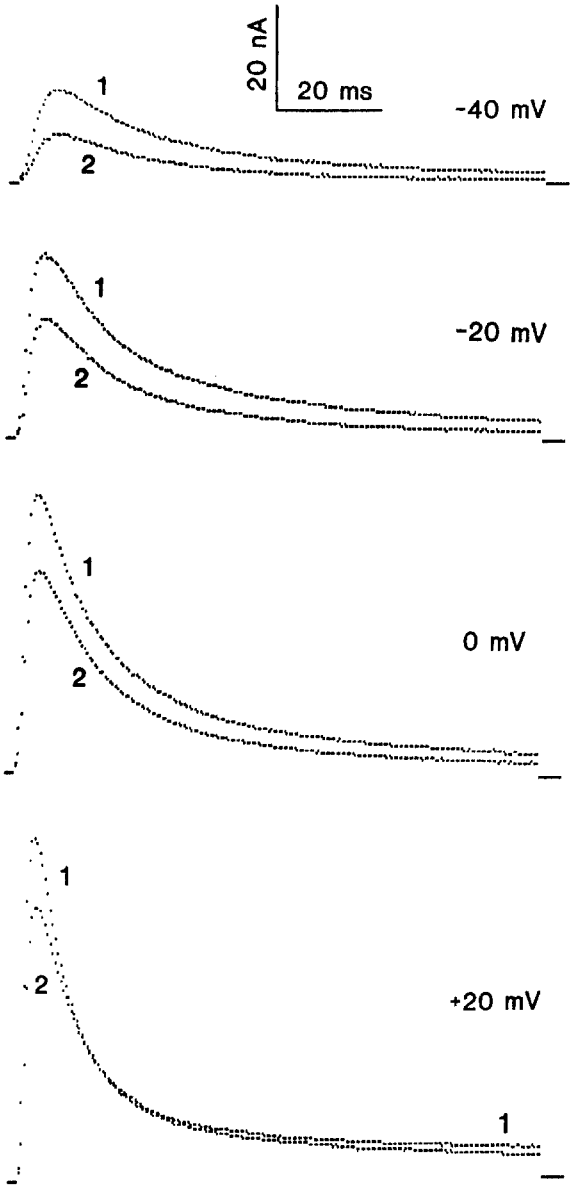

Fig. 7. The effect of 20 mM external TEA on the fast-inactivating A-current. Superimposed traces show currents recorded in the absence (traces 1) and presence (traces 2) of TEA in the external solution (solutions N1 and N2, respectively) at various depolarizing test potentials indicated. Test pulses were preceded by the conditioning hyperpolarization of −150 mV for a duration of 200 msec.

"crossover" of the current traces in the presence and absence of TEA. A slow decrease in the current amplitude and in the rate of inactivation are possibly due to slow TEA diffusion towards the internal mouth of the potassium channels. Figures 8*A* and 8*C* show current records before and 20 min after the start of the intracellular exposure with 20 mM TEA. The current traces recorded at different periods of TEA exposure cross over at the same point. Unfortunately, these experiments do not permit evaluation of the binding constant for TEA to A-channels, as the intracellular concentration of TEA is unknown during the various perfusion periods. However, this is not critical for modeling the TEA effect on a channel as the kinetic schemes used do not include the binding constants.

Achieving a balanced TEA concentration inside the cell is basically possible during a prolonged perfusion. This takes about 50–60 min. But by this time there is a drop in the potassium current in controls, and this could lead to an inaccurate estimation of the current blockade at exposures over 40 min.

The extent of channel blockade, as manifested in reduced current amplitude, depended on the potential exhibiting crossover of the current-voltage relations (Fig. 9). This effect results from the negative shift of the steady-state activation curve (by approximately 10 ± 3 mV after 20 min and 30 ± 5 mV after 40 min TEA exposures). Prolonged perfusion without TEA does not

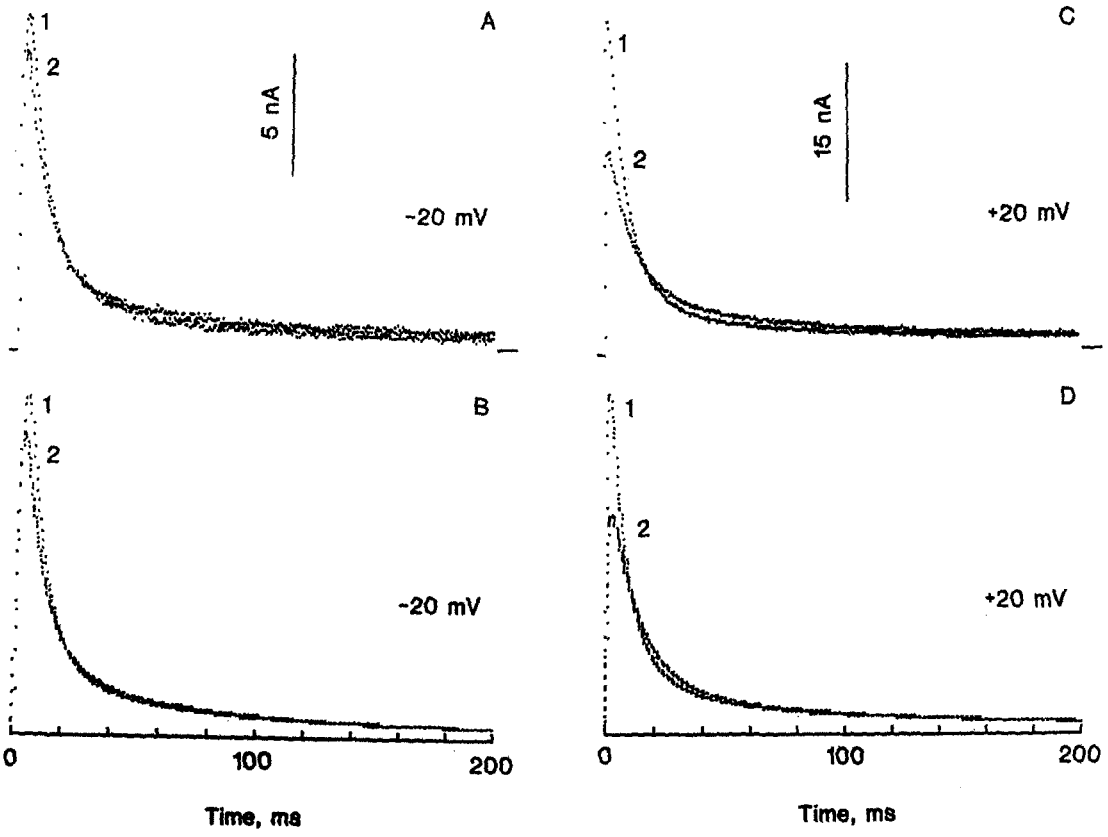

Fig. 8. The effect of 20 mM TEA on the fast-inactivating A-current after 20 min intracellular exposure. Superimposed traces show currents recorded in the internal control solution without TEA (traces 1) and in the presence of TEA (traces 2). Depolarizing test potentials of −20 mV (*A*) and +20 mV (*C*) were preceded by the conditioning hyperpolarization of −150 mV for a duration of 200 msec. *B,D:* TEA blockade of I_{af} at depolarizing test potentials −20 mV (*B*) and +20 mV (*D*) as computed using scheme 6.

result in statistically significant shifts (±5 mV) of this curve. The dependence of the rate constants of the fast phase of inactivation on the potential is shown in Fig. 10. The fast phase of inactivation virtually loses sensitivity towards the changes in the membrane potential in the range over 0 mV. At the same time, the slow components of inactivation are changed slightly.

The effect of intracellular TEA on the slow-inactivating current is different from the TEA effect on I_{af}. Within approximately the same period of perfusion with an intracellular solution containing 20 mM TEA, the decrease in the current amplitude was greater than in the case with I_{af} (Fig. 11). This means that the slow-inactivating current displays a greater sensitivity towards TEA than I_{af}. Moreover, TEA blockade does not lead to the crossover of the slow-inactivating current traces at any of the studied potentials for current record lengths of up to 1000 msec. The changes in the rate constants of both inactivation components were small. Also, the current decrease with time is nonuniform, which is also different from the effect of external TEA (Choi et al., 1991). The decrease of the current can be explained by the drop in the ratio of the pre-exponential coefficients of

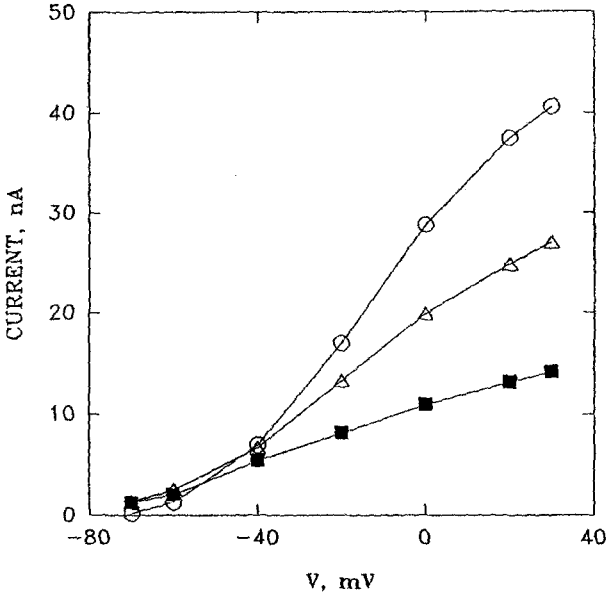

Fig. 9. Peak current-voltage relation of I_{af} without TEA in the internal solution (open circles) and after 20 min (open triangles) and 40 min (filled squares) intracellular exposure with 20 mM TEA.

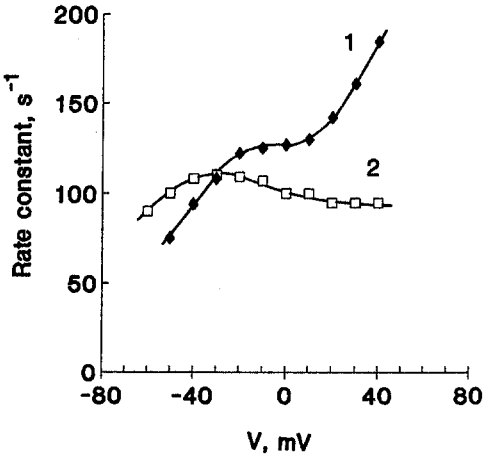

Fig. 10. Voltage dependence of the rate constants of the fast phase of inactivation ($1/\tau_f$) of I_{af} before (1) and after 20 min (2) of intracellular application of 20 mM TEA. The external medium contained 20 mM TEA (solution N2).

the fast and slow phases from 2 in the control to 1 in the presence of TEA. The external and internal TEA exposures caused the shifts of the steady-state activation and inactivation curves similar to those of I_{af}.

Discussion

Kinetic Model of Activation

If the inactivation process is coupled to the activation process it is difficult to derive true activation kinetics from the macroscopic current records. To find the activation rate constants satisfying the experimental data we performed the following calculations. First, we developed a kinetic model which describes the $I(t)/h(t)$ kinetics considering that activation and inactivation processes are independent. This model was used as a framework for a development of a full kinetic model of the channel including both activation and inactivation. Then, the calculated rate constants were modified in order to correspond the full model (Schemes 6,7) to rising phases and amplitudes of the current.

For describing the activation kinetics we have used a linear kinetic scheme equivalent to the HH n^4 model:

$$C_1 \underset{b_1}{\overset{a_1}{\rightleftharpoons}} C_2 \underset{b_2}{\overset{a_2}{\rightleftharpoons}} C_3 \underset{b_3}{\overset{a_3}{\rightleftharpoons}} C_4 \underset{b_4}{\overset{a_4}{\rightleftharpoons}} O \qquad \text{Scheme 1}$$

where C_1, C_2, C_3 and C_4 are the closed states of the channel, O is the open state, a_n are the forward rate constants, and b_n are the backward rate constants. The rate constants for such a model are usually assumed to depend exponentially on membrane potential V and given by $a_1 = 4\alpha$, $a_2 = 3\alpha$, $a_3 = 2\alpha$, $a_4 = \alpha$, $b_1 = \beta$, $b_2 = 2\beta$, $b_3 = 3\beta$, $b_4 = 4\beta$. α and β are defined in the expressions:

$$\alpha = \alpha_0 \exp(A_o V) \text{ and } \beta = \beta_0 \exp(-B_o V) \qquad (3)$$

where α_0 and β_0 are the rates at $V = 0$ mV of α and β, respectively. A_o and B_o specify the voltage dependencies of the rate constants α and β. The time course of probability for a channel to be in an open state, $P(t)$, can be found by solving the set of ordinary differential equations (Alekseev & Zaykin, 1993) describing this scheme. Because the instantaneous current-voltage relation is linear over the voltage range of −60 to +30 mV the conductance of a single A-channel, g, seems to be voltage independent at these potentials. Hence, the macroscopic current can be expressed as:

$$I(t) = Ng\ (V - E_r)\ P(t), \qquad (4)$$

where N is the number of channels, and E_r is the reversal potential (Zagotta & Aldrich, 1990). The equilibrium probability of residing in an open state, equal to $G(V)/G_{max}$, is given by the following equation:

$$P(\infty) = \left(1 + \sum_{j=1}^{4} \left\{ \prod_{i=j}^{4} (a_i/b_i) \right\} \right)^{-1} \qquad (5)$$

The theoretically obtained activation and deactivation kinetics were again approximated by corresponding exponentials and the results were compared with the experimental data. The calculation was assumed to be satisfactory if an acceptable fit was obtained to the three activation parameters $\tau_a(V)$, $\tau_d(V)$ and $G(V)/G_{max}$, and to the $I(t)/h(t)$ and deactivation kinetics at different values of V. Experiments with different concentrations of Ca^{2+} and Mg^{2+} imposed rigid limits on the choice of parameters of the kinetic scheme. Apparently, the fact that these ions do not affect the deactivation kinetics means that they have a small effect on the backward rate constants, whereas their effect on the forward rate constants is great. The use of the above-mentioned relationships between a_n and α (b_n and β) did not yield a satisfactory fit of the model to the observed kinetics. But a modification of the expressions for a_3 and a_4 led to reasonable agreement between theory and all the results. To achieve a good agreement between full model of the channel (Schemes 6,7) and the kinetics it was enough to make only small corrections of the pre-exponential coefficients in expression for α and a_3. The final values determined for the rate constants satisfying the various conditions of the experimental data are given in Table 2.

The fits of model to the deactivation kinetics and rising phases of currents are illustrated in Figs. 3 and 6, respectively. The function $P(\infty)$ is shown in Fig. 5.

The kinetic model of activation of *Lymnaea* A-cur-

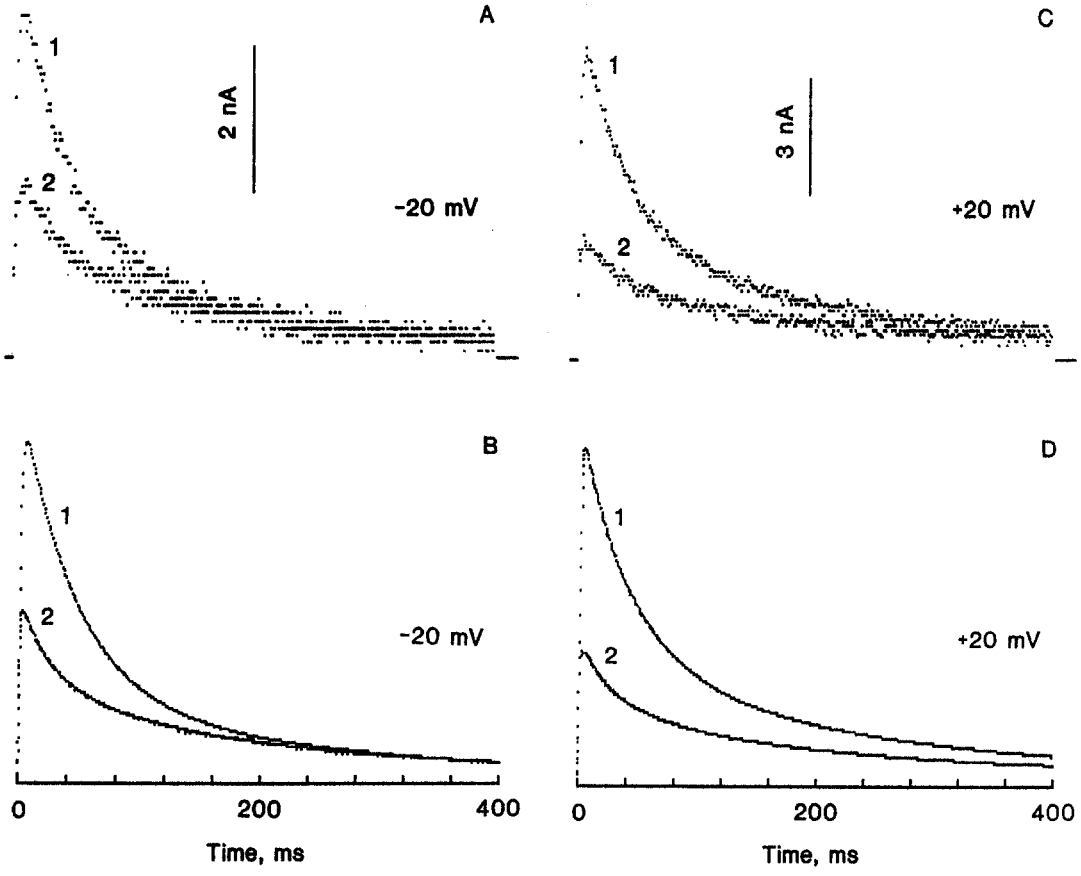

Fig. 11. The effect of 20 mM TEA on the slow-inactivating A-current after 20 min intracellular exposure. Superimposed traces show currents recorded in the absence (traces 1) and presence (traces 2) of TEA in the internal solution at depolarizing test potentials of −20 (*A*) and +20 mV (*C*) preceded by the conditioning hyperpolarization of 200 msec duration to −150 mV. The external solution contained 20 mM TEA (solution N2). *B,D:* Modeling of the TEA blockade of I_{as} at depolarizing test potentials of −20 mV (*B*) and +20 mV (*D*). The computer model used the kinetic scheme 7.

Table 2. The rate constants of kinetic scheme 1 used for modeling the activation kinetics under various experimental conditions

Parameter	2 mM Ca[a]	16 mM Ca[b]
a_1	4α	4α
a_2	3α	3α
a_3	2α/0.95	2α/1.4
a_4	α/2.1	α/7.7
b_1	β	β
b_2	2β	2β
b_3	3β	3β
b_4	4β	4β
α	1510 exp (0.025V)	1510 exp (0.025V)
β	10 exp (−0.027V)	10 exp (−0.027V)

[a] External solution N3; [b]External solution N4.

rents is similar to the one offered by Zagotta and Aldrich (1990) for *Shaker* A-type potassium channels in *Drosophila* muscles except for the fast voltage-independent transition introduced by the authors for describing the bursting activity of the channel. As the rate constants of this transition can not be calculated from the macroscopic current kinetics, we did not include it in our model. It should be noted that the obtained results do not agree with the HH model. As is shown in Table 2, this is conditioned by a considerable deviation of the rate constant of the last transition (α/2.1) from the one expected from the HH model (α). With increasing calcium concentration in the outer solution, this deviation becomes more obvious.

The effect of divalent ions on the activation kinetics and on the $G(V)/G_{max}$ curve can be explained either by the nonspecific screening of the fixed negative charge of the membrane surface (Frankenhaeuser & Hodgkin, 1957; Hanin & Campbell, 1983; McLaughlin, Sabo, & Eisenman, 1971) or by the specific binding of these cations to some negatively charged groups of the channel protein or to electrically close phospholipids (Hille, Woodhull, & Shapiro, 1975; Shoukimas, 1978; Gilly & Armstrong, 1982*a;* Gilly & Armstrong, 1982*b;* Mayer & Sugiyama, 1988). According to the Grahame equation (Grahame, 1947), the substitution of one solution (N3)

for another one (N4) of equal total ion charge concentration cannot cause a change in the membrane surface potential due to nonspecific screening of the surface negative charge. Since the total concentration of mono- and divalent ions was the same in both solutions, the shifts of the $G(V)/G_{max}$ and $\tau_a(V)$ curves could be caused only by a specific binding of divalent cations to negatively charged groups related to the channel protein. As the observed shifts have taken place with an increase of the concentration of calcium rather than magnesium, it can be concluded that specific binding of Ca^{2+} to negatively charged groups of the activation gate is the primary cause for these effects.

It should be noted that the specific Ca^{2+} binding to negatively charged groups of the activation gating apparatus does not influence the kinetics of deactivation. A similar result was obtained earlier for sodium and potassium channels of squid axons (Gilly & Armstrong, 1982*a;* Gilly & Armstrong, 1982*b*). Gilly and Armstrong (1982*a,b*) have suggested that the negatively charged element of the gating apparatus during activation moves from the resting position at the outer surface to the activated position at the inner surface of the membrane. Electrostatic attraction between gating charge and calcium ions stabilizes the gating charge at its resting position thereby decreasing the transition rate from the closed state to the open state. In the activated position, external calcium ions do not interact with gating charge and do not influence the backward rate constants. Such an interpretation of the calcium effect agrees with our data as well. This is especially evident in the kinetic model, where the effect of calcium is reproduced by reducing the rate constants of only forward, and not backward, transitions.

The effective valency of a gating particle controlling the kinetics of A-currents can be calculated by the following equations (Mayer & Sugiyama, 1988; Zagotta & Aldrich, 1990):

$$Z_a = A_o RT/F, \text{ and } Z_b = B_o RT/F \quad (6)$$

where A_o and B_o are coefficients determined from equations 3, R is the universal gas constant, T is the absolute temperature, F is the Faraday constant. For forward transitions, $Z_a = 0.64$, and for reverse ones, $Z_b = 0.69$. This corresponds to an equivalent charge movement of 1.33 electronic charges.

A comparative analysis of the activation parameters of fast- and slow-inactivating currents shows that both types of currents have equal kinetics and steady-state activation parameters and are apparently activated by the same mechanism. This provides support for assuming that A-channels in *Lymnaea* neurons are identical in the type of their activation gates, but differ in their inactivation mechanisms.

Kinetic Model of Inactivation of I_{af}

Inactivation of I_{af} in *Lymnaea* neurons in many instances is similar to that of fast inactivating K^+ currents in other cells and primarily to *Shaker* K^+ current (Alekseev & Zaykin, 1993). Experiments with TEA provides further confirmation of the similarity of the inactivation mechanisms of these types of channels. Like inactivation of *Shaker* K^+ channels (Choi et al., 1991), fast inactivation of I_{af} is slowed down by internal rather than external application of TEA. This effect can be explained by competition between TEA and the inactivation particle for binding to the same site on the internal mouth of the channel, indicating that the fast inactivation process appears to be due to a ball-and-chain mechanism (Armstrong & Bezanilla, 1977; Bezanilla & Armstrong, 1977; Hoshi et al., 1990; Zagotta et al., 1990; Hoshi et al. 1991). At the same time, TEA does not affect the rates of slower phases of inactivation. It can be inferred that the slower phases of inactivation do not involve ball-and-chain type mechanisms. As many features of the slow components are similar to C-type inactivation of *Shaker* potassium channels (Hoshi et al., 1990; Zagotta et al., 1990; Hoshi et al., 1991), it is reasonable to assume that a C-type mechanism is also the basis for slow inactivation of I_{af}.

Previous studies showed that inactivation of I_{af} has some specific differences which have not been revealed in other types of K^+ channels (Alekseev, 1992; Alekseev & Zaykin, 1993). It was found that the inactivation rate of the macroscopic current rises steeply with depolarization, except within the potential range from –30 to 0 mV, where the inactivation rate is maintained at a constant level. The $\gamma_f(V)$ curve exposes the pronounced plateau in this range (*see,* e.g. Fig. 10). Calcium ions affect the fast phase of inactivation only in the potential range from –70 to –20 mV producing a positive shift of a part of the $\gamma_f(V)$ curve on the left of the plateau. Raising the pH causes a negative shift of the right-hand branch of the $\gamma_f(V)$ curve. These effects can be described by using a model with at least two distinct voltage-dependent pathways for fast inactivation. Calcium and hydrogen ions are assumed to selectively affect the voltage-dependent transitions related to these pathways of inactivation (Alekseev & Zaykin, 1993).

Recently, the multiple inactivation process in the *Shaker* potassium channels was successfully described by partially coupled kinetic schemes (Zagotta & Aldrich 1990, Hoshi et al., 1991). The kinetic properties of I_{af} also allow us to model the gating of this channel on the basis of kinetic schemes suggested by Hoshi et al. (1991) and Zagotta and Aldrich (1990). We modified these schemes so as to describe the complex voltage dependence of fast inactivation. Three types of schemes are able to reproduce a rate-limiting process of fast inactivation occurring in the potential range of –30 to 0 mV:

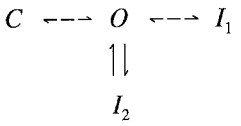

Scheme 2

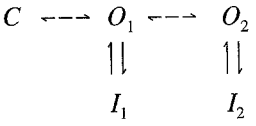

Scheme 3

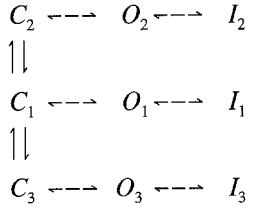

Scheme 4

In these schemes $C \leftrightarrows O$ transitions represent the set of activation transitions from the closed states to open ones. All transitions to inactivated states, I_i ($i = 1, 2, 3$), except transition $O \leftrightarrows I_2$ in scheme 2 are voltage independent. In schemes 2 and 3, transitions from an open state to an inactivated one, I_1, describe fast inactivation at $V \leqslant 0$ mV. Two additional transitions from an open state to I_2 are introduced for modeling fast inactivation at $V > 0$ mV. In this case, the voltage dependence of fast inactivation arises from the voltage-dependent transitions $O \leftrightarrows I_2$ in scheme 2 or $O_1 \leftrightarrows O_2$ in scheme 3. Both schemes satisfactorily described the effects of Ca^{2+} and H^+ on fast inactivation of I_{af} (Alekseev & Zaykin, 1993). We tried to reproduce a crossover of the current records caused by TEA blockage by introducing in these schemes an additional transition from an open state to a blocked one according to a competition model (Beam, 1976; Yeh & Narahashi, 1977; Cahalan, 1978; Neher & Steinbach, 1978; Cahalan & Almers, 1979; Grissmer & Cahalan, 1989; Choi et al., 1991). The first scheme did not adequately describe the changes caused by TEA in potential dependence of the fast phase of inactivation at $V > 0$ mV. Nor did the second scheme, with two successive open states, show a good correlation with the observed TEA effect on the current amplitude throughout the potential range studied. These results suggest that, first, transitions from open to inactivated states seem to be voltage-independent and, second, a channel has at least two independent open states. TEA blocks a channel whether it is in an open state at $V < 0$ mV or in a different open state at $V > 0$ mV.

Scheme 4 entirely satisfies these requirements. In this scheme, all three open states are independent and provide three pathways for inactivation. The first pathway describes fast inactivation at $V \leqslant -30$ mV. The second pathway is necessary for modeling the plateau in the $\gamma_f(V)$ curve. The third pathway describes the potential dependence of the fast phase of inactivation in the potential range greater than 0 mV. This scheme allows us to model the TEA blockade in different potential ranges independently introducing additional transitions from open states to blocked ones.

For detailed calculations of the kinetic parameters of inactivation and TEA blockade we used scheme 6 (*see* Appendix). The agreement of the model with the inactivation kinetics in control and in the presence of TEA is illustrated in Fig. 1*A* and Fig. 8, respectively.

The transitions of the channel from closed states to inactivated ones in scheme 6 are necessary for adequately describing the kinetics in the range from –90 to –60 mV. The rate constants of these transitions are equal to those used for describing the slower phases of inactivation. Hence, the model predicts that inactivation from the closed states involves the molecular mechanisms similar to those underlying slower inactivation. The channel being in a closed state can undergo this type of inactivation at early stages of activation. At the same time, fast inactivation can occur only from the open state of the channel which is in agreement with published data (Armstrong & Bezanilla, 1977; Bezanilla & Armstrong, 1977; Hoshi et al., 1990; Zagotta et al., 1990; Hoshi et al., 1991). These results are in line with suggestions of the different mechanisms underlying fast and slow inactivation of I_{af} channels.

We tested the effect of Ca^{2+} on the inactivation kinetics in scheme 6 by replacement of the activation rate constants calculated for solution N3 (Table 2) with those obtained for solution N4. The effect of H^+ on the fast phase of inactivation at $V > 0$ mV described earlier (Alekseev & Zaykin, 1993) was tested by changing the magnitudes of the rate constants δ_2 and σ_2 equivalent to a corresponding voltage shift. The model accurately reproduced both of these effects of calcium (Fig. 6) and H^+ (*data not shown*).

Kinetic Model of I_{as}

When developing a kinetic scheme for the slow-inactivating current, we took into account the following features of this current. I_{af} and I_{as} are activated in a similar way. The inactivation kinetics of I_{as} are similar to the slow phases of inactivation kinetics of I_{af}. Proceeding from this, we modified scheme 6 by removing the transitions responsible for the fast phase of inactivation and the whole third pathway responsible for fast inactivation in the potential range from 0 mV. The absolute magnitudes of the potential independent rate constants (s^{-1}) satisfying the inactivation kinetics of I_{as} are shown in scheme 7. The potential dependent rate constants are marked with letters corresponding to similar rate constants given for scheme 6. Examples of fit of current traces calculated numerically from scheme 7 to current records are shown in Fig. 1*B*.

The TEA effect was modeled by including new transitions from open states O_1 and O_2 into blocked states B_1 and B_2. The agreement with experimental data became possible only upon the introduction of two additional transitions similar to those for inactivation from a blocked state into an inactivated one. Calculated currents demonstrating the TEA effect are shown in Fig. 11*B,D*. These results show that a purely competitive model cannot be used to describe I_{as} blockade by TEA. It means that inactivation of the I_{as} channels does not seem to involve a ball-and-chain mechanism and is most likely to be similar to C-type inactivation of the *Shaker* potassium channels. The stronger blocking effect of TEA on I_{as} channel in this case could be explained by the absence of interference with an inactivation particle for binding with the channel.

Heteromultimeric Channel Hypothesis

Models for I_{af} and I_{as} channels formally developed on the basis of the kinetic data could be interpreted in terms of subunit composition of the channels. Recent studies have demonstrated that potassium channels can be formed by association of 4 identical (MacKinnon, 1991) or different subunits within a single subfamily (Christie et al., 1990; Isakoff, Jan, & Jan, 1990; Ruppersberg et al., 1990; Sheng et al., 1993; Wang et al., 1993). Each subunit contains an S4 segment, which can serve as a voltage sensor (Catterall, 1988; Jan & Jan, 1989). When depolarizing pulses are applied, the sensors reach a permissive state through conformational transitions before the channel can open. There are data supporting the fact that individual voltage sensors gate cooperatively (Tytgat & Hess, 1992). Activation schemes based upon independent gating of 4 identical subunits can adequately describe the kinetic properties of *Shaker* potassium channels (Zagotta, Hoshi, & Aldrich, 1994). These schemes include one open state indicating that a channel undergoes several conformational transitions before reaching the only conformation for open state.

The model developed in this paper for the I_{af} channel predicts the presence of three pathways of potential dependent conformational transitions of the channel to the open state. The conformation of the channel in each of these states is critical for inactivation. The transitions responsible for the inactivation gating do not depend on the potential. The potential dependence of the inactivation kinetics results entirely from the potential dependence of the activation gate. The inactivation rates accelerate as activation progresses. This is also confirmed by the experimental result showing that the shift of the normalized conductance curve produced by Ca^{2+} is followed by the same shift of a part of the $\gamma_f(V)$ curve on the left of the plateau. The complex behavior of the inactivation kinetics could be explained on the basis of a monomultimeric or a heteromultimeric assembly of the channels. Two branches of the $\gamma_f(V)$ curve separated by the plateau could be reproduced by at least two types of monomultimeric channels provided that their normalized conductances are shifted by about 30 mV (width of the plateau) relative to each other. However, experimental results have not revealed any such complex normalized conductance curve. This gives reason to assume that *Lymnaea* A-channels are probably arranged as heteromultimers, and not as monomultimers. In this case some diversity in the individual electrical properties (charge, dipole moment, etc.) of the different subunits could result in more complicated conformational changes of the channel. We can assume that some of the subunits at different membrane potentials selectively affect the direction of the conformational changes of the channel to open state according to their electrical properties.

We can offer several explanations for the difference between the slow- and fast-inactivating channels. First, the composition of subunits in the I_{as} channel may be different from that of I_{af} channel. Second, the difference in the mechanism of slow inactivation could be due to differences in the structure of some parts of the channel protein, such as in the NH_2-terminus, preventing the channel from inactivation by a ball-and-chain mechanism. It is also possible that the lipid environment of the channel, or of other natural components of the neuronal membrane, may be capable of modifying the channel gating. The physiological significance of slow-inactivating potassium channels remains to be determined.

We thank Dr. L.W. Horn for suggestions and comments and Emma Kapiliovich for secretarial assistance in the preparation of this manuscript. We gratefully acknowledge the financial support of the Richard J. Fox Foundation and the National Academy of Science (USA) through the CAST Program.

References

Alekseev, S.I. 1992. Interaction of sulfhydryl reagents with A-type channels of *Lymnaea* neurons. *Biochim. Biophys. Acta* **1110**:178–184

Alekseev, S.I., Zaykin, A.V. 1993. Kinetic study of A-type current inactivation in *Lymnaea* neurons. *Biochim. Biophys. Acta* **1148**:97–107

Armstrong, C.M., Bezanilla, F. 1977. Inactivation of the sodium channel. II. Gating current experiments. *J. Gen. Physiol.* **70**:567–590

Armstrong, C.M., Binstock, L. 1965. Anomalous rectification in squid giant axon injected with tetraethylammonium chloride. *J. Gen. Physiol.* **48**:859–872

Armstrong, C.M., Hille, B. 1972. The inner quaternary ammonium ion receptor in potassium channels of the node of *Ranvier*. *J. Gen. Physiol.* **59**:388–400

Beam, K.G. 1976. A quantitative description of end-plate currents in the presence of two lidocaine derivatives. *J. Physiol.* **258**:301–322

Bezanilla, F., Armstrong, C.M. 1977. Inactivation of the sodium channel. I. Sodium current experiments. *J. Gen. Physiol.* **70**:549–566

Cahalan, M.D. 1978. Local anesthetic block of sodium channels in normal and pronase-treated squid axons. *Biophys. J.* **23**:285–311

Cahalan, M.D., Almers, W. 1979. Block of sodium conductance and gating current in squid giant axons poisoned with quarternary strychnine. *Biophys. J.* **27**:57–74

Catterall, W.A. 1988. Structure and function of voltage-sensitive ion channels. *Science* **242**:50–61

Choi, K.L., Aldrich, R.W., Yellen, G. 1991. Tetraethylammonium blockade distinguishes two inactivation mechanisms in voltage-activated K^+ channels. *Proc. Natl. Acad. Sci. USA* **88**:5092–5095

Choi, K.L., Mossman, C., Aube, J., Yellen, G. 1993. The internal quaternary ammonium receptor site of *Shaker* potassium channels. *Neuron* **10**:533–541

Christie, M.J., North, R.A., Osborne, P.B., Douglass, J., Adelman, J.P. 1990. Heteropolymeric potassium channels expressed in *Xenopus* oocytes from cloned subunits. *Neuron* **4**:405–411

Frankenhaeuser, B., Hodgkin, A.L. 1957. The action of calcium on the electrical properties of squid axons. *J. Physiol.* **137**:218–244

Gilly, W.F., Armstrong, C.M. 1982*a*. Divalent cations and the activation kinetics of potassium channels in squid giant axons. *J. Gen. Physiol.* **79**:965–996

Gilly, W.F., Armstrong, C.M. 1982*b*. Slowing of sodium channel opening kinetics in squid axon by extracellular zinc. *J. Gen. Physiol.* **79**:935–964

Grahame, D.C. 1947. The electrical double layer and the theory of electrocapillarity. *Chem. Rev.* **41**:441–501

Grissmer, S., Cahalan, M. 1989. TEA prevents inactivation while blocking open K^+ channels in human T lymphocytes. *Biophys. J.* **55**:203–206

Hahin, R., Campbell, D.T. 1983. Simple shifts in the voltage dependence of sodium channel gating caused by divalent cations. *J. Gen. Physiol.* **82**:785–802

Hille, B., Woodhull, A.M., Shapiro, B.I. 1975. Negative surface charge near sodium channels of nerve: divalent ions, monovalent ions, and pH. *Phil. Trans. Roy. Soc. London* **270**:301–318

Hodgkin, A.L., Huxley, A.F. 1952. A quantitative description of membrane current and its application to conduction and excitation in nerve. *J. Physiol.* **117**:500–544

Hoshi, T., Zagotta, W.N., Aldrich, R.W. 1990. Biophysical and molecular mechanisms of *Shaker* potassium channel inactivation. *Science* **250**:533–538

Hoshi, T., Zagotta, W.N., Aldrich, R.W. 1991. Two types of inactivation in *Shaker* K^+ channels: effects of alterations in the carboxy-terminal region. *Neuron* **7**:547–556

Isakoff, E.Y., Jan, Y.N., Jan, L.Y. 1990. Evidence for the formation of heteromultimeric potassium channels in *Xenopus* oocytes. *Nature* **345**:530–534

Jan, L.Y., Jan, Y.N. 1989. Voltage-sensitive ion channels. *Cell* **56**:13–25

Keynes, R.D., Rojas, E. 1976. The temporal and steady-state relationships between activation of the sodium conductance and movement of the gating particles in the squid giant axons. *J. Physiol.* **255**:157–189

MacKinnon, R. 1991. Determination of the subunit stoichiometry of a voltage-activated potassium channel. *Nature* **350**:232–234

Mayer, M.L., Sugiyama, K. 1988. A modulatory action of divalent cations on transient outward current in cultured rat sensory neurones. *J. Physiol.* **396**:417–433

McLaughlin, S.G.A., Sabo, G., Eisenman, G. 1971. Divalent ions and the surface potential of charged phospholipid membrane. *J. Gen. Physiol.* **58**:667–687

Neher, E., Steinbach, J.H. 1978. Local anesthetics transiently block currents through single acetylcholine-receptor channels. *J. Physiol* **277**:153–176

Oxford, G.S. 1981. Some kinetic and steady-state properties of sodium channels after removal of inactivation. *J. Gen. Physiol.* **77**:1–22

Ruppersberg, J.P., Schroter, K.H., Sakmann, B., Stocker, M., Sewing, S., Pongs, O. 1990. Heteromultimeric channels formed by rat brain potassium-channel proteins. *Nature* **345**:535–537

Sheng, M., Liao, Y.J., Jan, Y.N., Jan, L.Y. 1993. Presynaptic A-current based on heteromultimeric K^+ channels detected *in vivo*. *Nature* **365**:72–75

Shoukimas, J.J. 1978. Effect of calcium upon sodium inactivation in the giant axons of *Loligo pealei*. *J. Membrane Biol.* **38**:271–289

Solc, C.K., Aldrich, R.W. 1990. Gating of single non-*Shaker* A-type potassium channels in Larval *Drosophila* neurons. *J. Gen. Physiol.* **96**:135–165

Tytgat, J., Hess, P. 1992. Evidence for cooperative interactions in potassium channel gating. *Nature* **359**:420–423

Wang, H., Kunkel, D.D., Martin, T.M., Schwartzkroin, P.A., Tempel, B.L. 1993. Heteromultimeric K^+ channels in terminal and juxtaparanodal regions of neurons. *Nature* **365**:75–79

Yeh, J.Z., Narahashi, T. 1977. Kinetic analysis of pancuronium interaction with sodium channels in squid axon membranes. *J. Gen. Physiol.* **69**:293–323

Yellen, G., Jurman, M.E., Abramson, T., MacKinnon, R. 1991. Mutations affecting internal TEA blockade identify the probable pore-forming region of a K^+ channel. *Science* **251**:939–942

Zagotta, W.N., Aldrich, R.W. 1990. Voltage-dependent gating of *Shaker* A-type potassium channels in *Drosophila* muscle. *J. Gen. Physiol.* **95**:29–60

Zagotta, W.N., Hoshi, T., Aldrich, R.W. 1990. Restoration of inactivation in mutants of *Shaker* potassium channels by a peptide derived from ShB. *Science* **250**:568–571

Zagotta, W.N., Hoshi, T., Aldrich, R.W. 1994. *Shaker* potassium channel gating III: Evaluation of kinetic models for activation. *J. Gen. Physiol.* **103**:321–362

Appendix

Scheme 4 was used as a basis for development of the detailed kinetic scheme (Scheme 6) of the A-channels. We assumed that the rate constants of transitions from the last closed states to open ones in all three pathways are the same. The conductance of the channel in the open states and the inactivation mechanisms involved are identical. According to Hoshi et al. (1991), the model describing three-exponential decay of the current can be formalized by the following kinetic scheme:

$$\begin{array}{ccccccc} C_1 & \longleftrightarrow & O_1 & \longleftrightarrow & I_{1s} & \longleftrightarrow & I_{2s} \\ & & \updownarrow & & & & \updownarrow \\ & & I_f & \longleftrightarrow & I_{1fs} & \longleftrightarrow & I_{2fs} \end{array} \qquad \text{Scheme 5}$$

The fast phase of inactivation is described by the transition from open to inactivated state, I_f; and the two slow phases by transitions from open state to successive inactivated states, I_{1s} and I_{2s}. In *Shaker* potassium channels slow inactivation is partially coupled with fast inactivation. This kinetic feature may be general for the fast inactivating potassium channels also. Therefore, we introduced into the model additional coupling inactivated states, similar to I_{1fs} and I_{2fs}.

The probability of the transition of the channel to the second or third activation pathway is determined by the voltage-dependent rate constants δ_1, σ_1 and δ_2, σ_2. Good agreement between model and experimental data was obtained using the following magnitudes of these rate constants (s^{-1}):

$$\delta_1 = 1000 \exp(+0.025\ V);\ \sigma_1 = 1000 \exp(-0.025\ V) \text{ and} \qquad \text{(A1)}$$

$$\delta_2 = 2700 \exp(+0.05\ V);\ \sigma_2 = 8970 \exp(-0.05\ V). \qquad \text{(A2)}$$

The calculated magnitudes of the rate constants of inactivation are shown in Fig. 12.

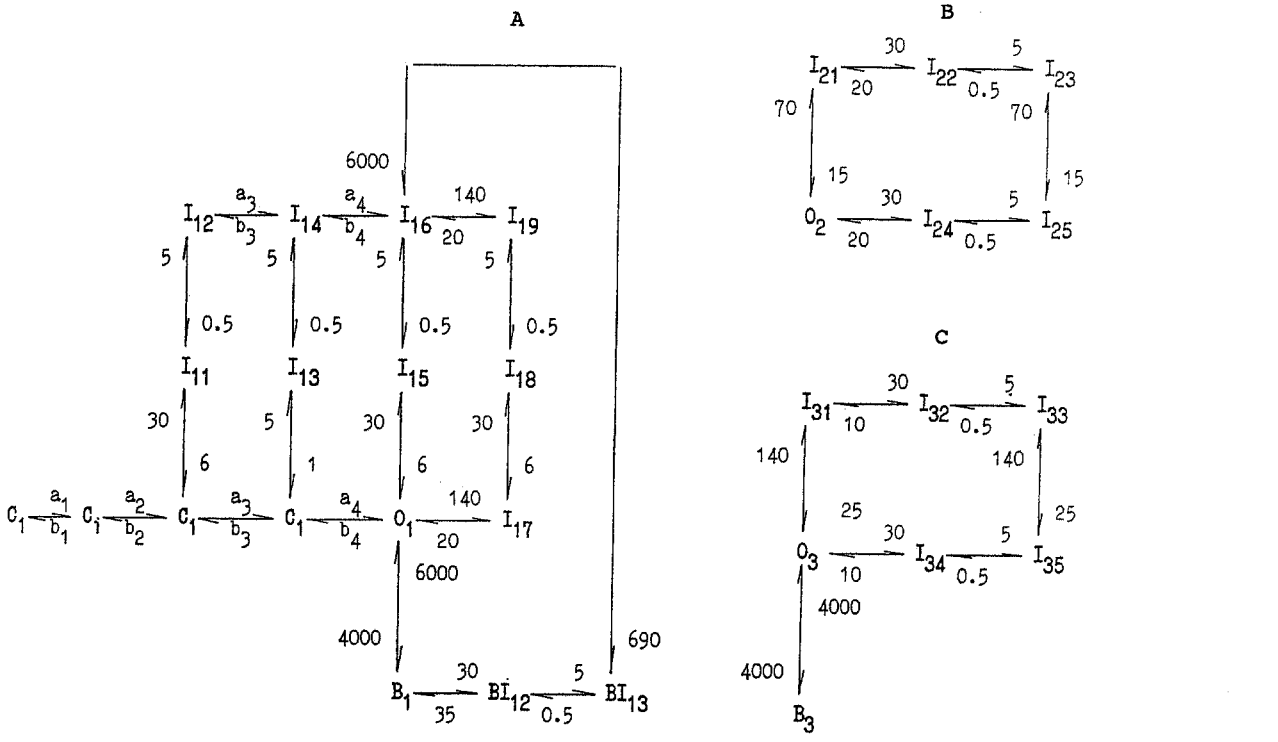

Fig. 12. The absolute magnitudes of the voltage-independent rate constants (s^{-1}) used in scheme 6 for the transitions to the negative- (*A*), mid- (*B*) and high- (*C*) voltage-range pathways, which fit all the parameters of I_{af}. The activation transition rates (a_n and b_n; n = 1,2,3,4) were equated to those shown in Table 2. TEA blockade was modeled by transition from the open (O_1) to blocked (B)$_1$ states in negative potential range and by transition from the open (O_3) to the blocked (B_3) state in the high potential range (> 0 mV).

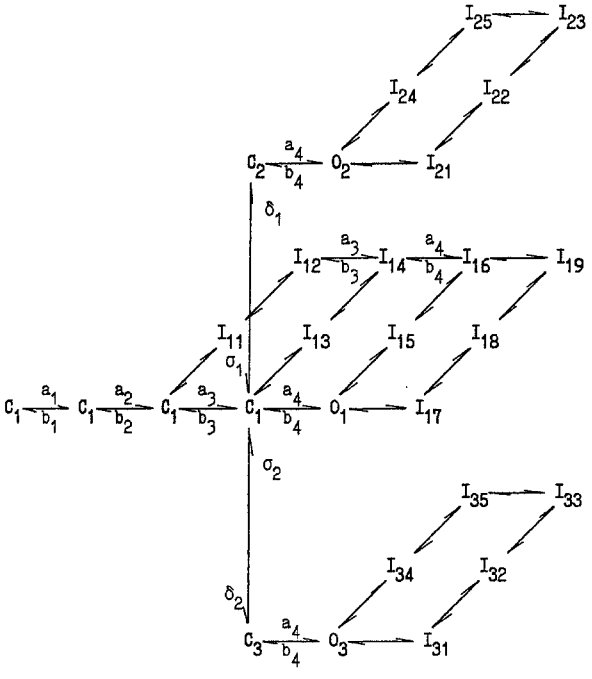

Scheme 6

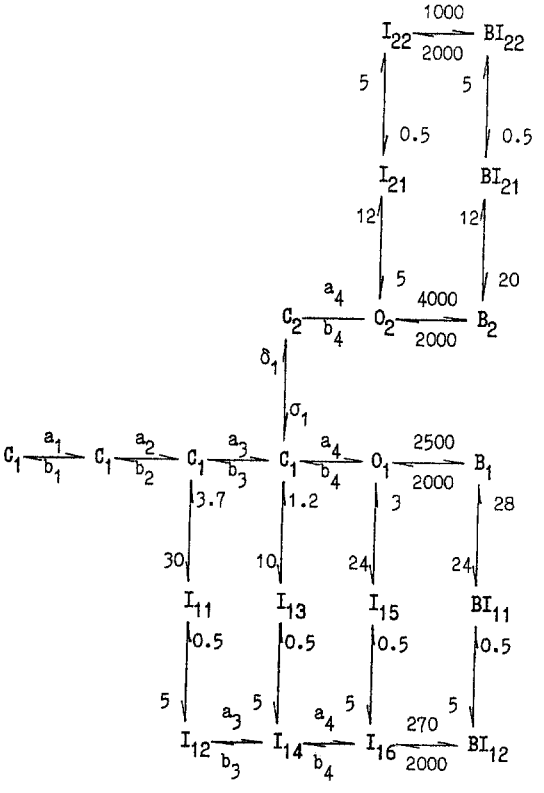

Scheme 7

Inactivation occurs more readily from the first open state, O_1, in the potential range from −90 to −30 mV, from the second open state, O_2, in the potential range from −30 to 0 mV, and from the third open state, O_3, at potentials over 0 mV. The rates of δ_1, σ_1 and δ_2, σ_2 at $V = 0$ were chosen arbitrarily so that the forward rates of δ_1 at $V > -30$ mV and δ_2 at $V > 0$ mV should exceed the rate of a_4. The number of closed states (C_1) prior to the $C_1 \rightarrow C_2$ or $C_1 \rightarrow C_3$ transitions is not critical; the results will be the same as long as the relative values of the forward rate constants for the transitions to the negative-, mid-, and high-voltage range pathways remain the same. The magnitudes of the backward rate constants of inactivation transitions I_{11}–I_{12}, I_{13}–I_{14}, etc., were less critical for calculated results. We consider that the accurate determination of these rate constants is possible only from single-channel recordings.

It should be noted that some transitions coupling slow inactivation with fast inactivation (I_{17}–I_{18}–I_{19}–I_{16}, I_{21}–I_{22}–I_{23}–I_{25}, I_{31}–I_{32}–I_{33}–I_{35}, I_{12}–I_{14}–I_{16}) are not essential for fitting of the model to the inactivation kinetics. We were able to reproduce all experimental results with the same scheme without these particular transitions. However, we decided to keep them in the kinetic scheme to depict more accurately the underlying physical processes.

The intracellular TEA blockade of I_{af} was described by a competition model. An acceptable agreement between the theoretical kinetics and the experimental data (Fig. 8*B,D*) was reached by introducing transitions from two open states O_1 and O_3 into blocked states B_1 and B_3, respectively (Fig. 12). The activation rate constants used in Scheme 6 were amended in order to correspond to the 10 mV negative shift caused by TEA. Moreover, to achieve a reasonable fit of the model to slow decaying phases of the current records, we included two additional transitions from blocked state B_1 with the rate constants close to those responsible for the slow phases of inactivation. Thus, the model predicts that slow inactivation can take place from a blocked state of the channel. TEA had a small effect on the rates of the slow components of inactivation. It seems that TEA does not interact with slow inactivation gating and, hence, TEA unblocking may be independent on the slow inactivation process. In Fig. 12 we indicated this possibility by transition $BI_{13} \rightarrow I_{16}$. This model accurately describes experimental results in the potential range from −30 to 0 mV without introducing an additional transition from O_2 to blocked state B_2, indicating that the degree of block from the O_2 state is very small. As can be seen, the ratio of the rate constants of forward and reverse transitions, which is proportional to the binding constant for TEA, is distinct for each of the three different blocked states. Hence, the channel conformation in the area of the intracellular receptor for TEA could differ in states O_1, O_2 and O_3 as well.